Glycine Transporter Type 1 Occupancy by Bitopertin: a Positron Emission Tomography Study in Healthy Volunteers

Meret Martin-Facklam*[1,6] , Flavia Pizzagalli[1,6], Yun Zhou[2], Susanne Ostrowitzki[1], Vanessa Raymont[2], James R Brašić[2], Nikhat Parkar[1], Daniel Umbricht[1], Robert F Dannals[2], Ron Goldwater[3] and Dean F Wong[2,4,5]

[1]Pharmaceutical Division, F. Hoffmann-La Roche, Basel, Switzerland; [2]The Russell H. Morgan Department of Radiology and Radiological Science, The Johns Hopkins University School of Medicine, Baltimore, MD, USA; [3]PAREXEL International, Baltimore, MD, USA; [4]Research Administration and Training, Department of Radiology, Psychiatry, Neuroscience and Environmental Health Sciences, The Johns Hopkins University School of Medicine, Baltimore, MD, USA; [5]Section High Resolution Brain PET Imaging, The Johns Hopkins University School of Medicine, Baltimore, MD, USA

Deficient N-methyl-D-aspartate (NMDA) receptor transmission is thought to underlie schizophrenia. An approach for normalizing glutamate neurotransmission by enhancing NMDA receptor transmission is to increase glycine availability by inhibiting the glycine transporter type 1 (GlyT1). This study investigated the relationship between the plasma concentration of the glycine reuptake inhibitor bitopertin (RG1678) and brain GlyT1 occupancy. Healthy male volunteers received up to 175 mg bitopertin once daily, for 10–12 days. Three positron emission tomography scans, preceded by a single intravenous infusion of ~ 30 mCi [^{11}C]RO5013853, were performed: at baseline, on the last day of bitopertin treatment, and 2 days after drug discontinuation. Eighteen subjects were enrolled. At baseline, regional volume of distribution (V_T) values were highest in the pons, thalamus, and cerebellum (1.7–2.7 ml/cm^3) and lowest in cortical areas (~ 0.8 ml/cm^3). V_T values were reduced to a homogeneous level following administration of 175 mg bitopertin. Occupancy values derived by a two-tissue five-parameter (2T5P) model, a simplified reference tissue model (SRTM), and a pseudoreference tissue model (PRTM) were overall comparable. At steady state, the relationship between bitopertin plasma concentration and GlyT1 occupancy derived by the 2T5P model, SRTM, and PRTM exhibited an EC$_{50}$ of ~ 190, ~ 200, and ~ 130 ng/ml, respectively. E_{max} was $\sim 92\%$ independently of the model used. Bitopertin plasma concentration was a reliable predictor of occupancy because the concentration–occupancy relationship was superimposable at steady state and 2 days after drug discontinuation. These data allow understanding of the concentration–occupancy–efficacy relationship of bitopertin and support dose selection of future molecules.

Neuropsychopharmacology (2013) 38, 504–512; doi:10.1038/npp.2012.212; published online 7 November 2012

Keywords: receptors; N-methyl-D-aspartate; glycine transporter 1; glycine reuptake inhibitor; bitopertin; RG1678; schizophrenia

INTRODUCTION

Deficient signaling through the N-methyl-D-aspartate (NMDA) receptor has been hypothesized to be a key factor underlying many signs and symptoms of schizophrenia (Javitt, 2007). Increasing NMDA receptor function pharmacologically is thought to compensate for hypofunctional receptor signaling and is an attractive approach for the treatment of schizophrenia. Targeting the allosteric glycine site of the NMDA receptor has been proposed as an approach to enhance NMDA receptor functioning and thus normalize glutamate transmission (Javitt, 2009). This can be achieved by using glycine agonists and also by preventing synaptic clearance of glycine through the inhibition of the glycine transporter type 1 (GlyT1). Support for this hypothesis is provided by non-clinical and clinical studies with full and partial agonists at the glycine site, and with sarcosine, a naturally occurring inhibitor of GlyT1 (Javitt, 2006).

A selective and potent glycine reuptake inhibitor (GRI), bitopertin (RG1678, F. Hoffmann-La Roche, Basel, Switzerland, [4-(3-fluoro-5-trifluoromethylpyridin-2-yl)piperazin-1-yl]-[5-methanesulfonyl-2-((S)-2,2,2-trifluoro-1-methylethoxy)phenyl]methanone) (Pinard et al, 2010), is currently in Phase III of clinical development. Bitopertin has demonstrated efficacy in preclinical assays of decreased NMDA receptor functioning and models of schizophrenia. In addition, it increases cerebrospinal fluid (CSF) glycine levels in a dose-dependent manner (Alberati et al, 2012). Correspondingly, in a proof-of-mechanism study in healthy volunteers, once-daily oral doses of 3–60 mg bitopertin over

10 days resulted in a dose-dependent increase in glycine levels in CSF of a similar magnitude (Hofmann et al, 2011).

RO5013853 (F. Hoffmann-La Roche, Basel, Switzerland, [5-methanesulfonyl-2-((S)-2,2,2-trifluoro-1-methyl-ethoxy)-phenyl]-[5-(tetrahydro-pyran-4-yl)-1,3-dihydro-isoindol-2-yl]-methanone), a selective and potent GRI that binds at the same site on GlyT1 as bitopertin, constitutes a promising agent for development as a clinical radioligand (Pinard et al, 2011). Rat autoradiographic studies showed that the distribution of the binding sites of [³H]RO5013853 corresponded to the known distribution of GlyT1 in the brain. Positron emission tomography (PET) in baboons showed rapid brain uptake of [¹¹C]RO5013853, with the highest uptake in brain stem, pons, thalamus, and cerebellum (Borroni et al, 2011). Scans carried out in healthy volunteers confirmed the ability of [¹¹C]RO5013853 to image regions expressing GlyT1. Test–retest variability for volume of distribution (V_T) was low (<10%), confirming that [¹¹C]RO5013853 may be used in occupancy studies (Wong et al, 2011).

The objectives of this study were to assess whether [¹¹C]RO5013853 binding in the brain can be displaced by bitopertin and to assess the relationship between bitopertin plasma concentration and brain GlyT1 occupancy at steady state and after bitopertin discontinuation.

MATERIALS AND METHODS

Study Design

This single-center study used an open-label, non-randomized, parallel-group design. The study was conducted in accordance with the Declaration of Helsinki Principles and approved by the Johns Hopkins Medicine Institutional Review Boards (Baltimore, MD, USA) and Chesapeake Research Review (Columbia, USA). Bitopertin (RG1678) was administered orally once daily for 10–12 days, to allow flexibility for scheduling of PET scanning. A first PET scan was performed at baseline (day −1), a second on the last day of treatment (4–12 h post-dose), and a third 2 days after the last dose. Subjects entered the clinic before the first scan and remained in-house until after the third scan. Subjects received a single intravenous short infusion (~30 s) of [¹¹C]RO5013853 immediately before each scan.

Bitopertin Doses

Subjects initially received 30 or 175 mg bitopertin once daily. The dose of 175 mg was chosen based on the highest dose tested in a multiple ascending-dose study to gain information on the maximum displacement of [¹¹C]RO5013853. The dose of 30 mg was estimated to reach half-maximal GlyT1 occupancy based on occupancy in baboons (Borroni et al, 2011). Because bitopertin was found to displace [¹¹C]RO5013853, further dose groups (5, 15, and 60 mg) were enrolled to describe the full dose–occupancy relationship. Bitopertin treatment duration was at least 10 days, which is sufficient time to reach steady state in line with the half-life of ~2 days. At steady state, the CSF concentration–time profiles were flat and with a constant plasma/CSF ratio between 4 and 12 h post dose (Hofmann et al, 2011).

Safety

Safety assessments were performed regularly and included monitoring of adverse events (AEs), vital signs, electrocardiogram (ECG) parameters, and routine laboratory tests.

Subjects

Healthy male volunteers were enrolled. All subjects were in good physical health as demonstrated by medical history, physical examination, vital signs, ECG, and routine laboratory tests. Subjects were excluded if they had a history of head trauma with prolonged loss of consciousness; a history of migraine headaches or neurologic conditions; implanted or embedded objects that would present a risk during magnetic resonance imaging (MRI); prior exposure to ionizing radiation such that study treatment would result in cumulative exposure exceeding recommended exposure limits. All subjects gave written, informed consent before entry to the study.

Radioligand [¹¹C]RO5013853

[¹¹C]RO5013853 was synthesized as previously described (Pinard et al, 2011). The injected radioactive dose, percent injected dose (injected tracer dose (mCi)/subject weight (kg)), mass dose and specific activity of all [¹¹C]RO5013853 scans were 29.45 ± 1.38 mCi, 0.381 ± 0.042 mCi/kg, 1.72 ± 0.92 µg, and 11360 ± 6293 mCi/µmol, respectively (mean $\pm$ SD, $N = 43$, excluding subjects with baseline scan only).

Input Function Measurement

An intravenous catheter was inserted into a vein in the antecubital fossa for [¹¹C]RO5013853 injection and an arterial catheter was placed in the radial artery at the contralateral wrist for blood sampling. Arterial blood samples were collected during each PET scan to determine total and metabolite-associated plasma radioactivity as described in Wong et al. (2011) and Hilton et al. (2000). The free fraction determined by earlier in vitro studies by equilibrium dialysis was 14.0% (SD 1.2).

The percentage of metabolites (ie, the radioactivity originating from metabolites of [¹¹C]RO5013853 over the total radioactivity) over 90 min was calculated by linear interpolation. The metabolite-corrected time–activity curve (TAC) was calculated as input function for compartmental model analysis using plasma input function.

Magnetic Resonance Imaging

Each subject underwent a limited diagnostic brain MRI scan as part of the screening procedures. Imaging was conducted on a GE Trio 3T Signa scanner. Images included a spoiled gradient-recalled (SPGR) acquisition in the steady-state sequence and double-echo (proton density and T2-weighted) sequence. The MRI from SPGR sequence was further used for co-registration with the PET data to enhance anatomical definitions of regions of interest (ROI).

PET Scan Procedures

PET scans were performed as described in Wong et al. (2011). Briefly, emission PET images were acquired on a GE Advance PET scanner. The 90 min dynamic emission scan acquired in three-dimensional mode started with radioligand injection over 1–2 min. Dynamic images were reconstructed using filtered back-projection with a ramp filter, resulting in a spatial resolution of $5.5 \times 5.5 \times 4.25$ mm full-width at half-maximum at the center of the field of view. Data in the decay-corrected, reconstructed, dynamic images were expressed in units of concentration (μCi/cm^3).

Image Analysis

The average of 90 min dynamic PET images were used for PET-to-PET registration and MRI-to-PET co-registration using statistical parametric mapping 2 software (Friston, 2002). The dynamic PET scans following treatment and MRI images were registered to the baseline PET scans for each subject. The ROI including cerebellum, pons, caudate, putamen, thalamus, and orbital frontal, entire prefrontal, superior frontal, occipital, temporal, parietal, cingulate cortices for gray matter, and centrum semiovale for white matter were manually drawn on the co-registered MRI images (Zhou et al, 2007). The ROI TACs were obtained by applying ROI to dynamic PET images. To enable comparisons between scans and subjects' tracer uptake without kinetic modeling, a semi-quantitative measurement called standardized uptake value (SUV) was calculated for ROI TACs:

$$\text{SUV(TAC)} = \text{TAC}\,(\mu\text{Ci/cm}^3)/(\text{injected tracer dose (mCi)/bodyweight (g)})$$

Tracer Kinetic Modeling

For compartmental modeling, a two-tissue five-parameter (2T5P) model in series configuration (Supplementary Figure S1; Innis et al, 2007) was used to fit the measured ROI TACs. Previous [^{11}C]RO5013853 studies in both baboons and humans have shown that a 2T5P model provides a better fit than a one-tissue three-parameter model. The 2T5P model assumes two tissue compartments for the ligand in the brain with five parameters: K_1 (ml/min/cm^3), the transport rate constant from vascular space to target tissue; k_2 (per min), the efflux rate constant from free plus nonspecific compartment to blood; k_3 (per min), the rate of specific receptor binding; k_4 (per min), the rate of dissociation from receptors; and V_P (ml/cm^3), the vascular volume in tissue. To reduce the variation of the tracer total distribution volume (V_T) resulting from the estimates of k_4, a non-linear model fitting algorithm with k_4 was coupled over ROIs for each dynamic PET study (Cunningham et al, 2004; Zhou et al, 2007; Zhou et al, 2010). V_T in tissue (ml/cm^3) was calculated after model fitting as $V_T = (K_1/k_2)(1 + k_3/k_4)$.

Once V_T was estimated, binding potential (BP$_{ND}$; Innis et al, 2007; Koeppe et al, 1991), an index of tracer-specific binding to receptors, was calculated as: $\text{BP}_{ND} = V_T/V_{T,ref} - 1$, where $V_{T,ref}$ was the V_T in the reference region (ie, superior frontal cortex).

To simplify PET data acquisition and quantification in the future, a simplified reference tissue model (SRTM) of three parameters (R_1, k_2, BP$_{ND}$, $R_1 = K_1/K_{1R}$) using reference tissue input was evaluated. The SRTM is based on the presence of a region without specific binding of the ligand (reference region; Lammertsma and Hume, 1996; Zhou et al, 2003), as illustrated in Supplementary Figure S1. For the compartmental model and SRTM, occupancy (Occ) was calculated as:

$$\text{Occ}\,(\%) = (\text{BP}_{ND}(\text{baseline}) - \text{BP}_{ND}(\text{blocking})) \times 100/\text{BP}_{ND}(\text{baseline})$$

Finally, a pseudoreference tissue model (PRTM; Gunn et al, 2011) was evaluated: $\text{Occ}\,(\%) = \text{Occ}^{2T5P} \times (1 + \text{BP}_{ND}(\text{reference tissue}))/(1 + \text{BP}_{ND}(\text{reference tissue}) \times \text{Occ}^{2T5P})$, where Occ^{2T5P} was occupancy (%) derived by 2T5P and BP$_{ND}$ (reference tissue) estimated by blocking studies using Lassen plots (Cunningham et al, 2010; Wong et al, 2000; Lassen et al, 1995).

Parametric Image of V_T

To evaluate voxel-wise tracer distribution in brain, a relative equilibrium-based graphical analysis with Patlak plot (Patlak et al, 1983; Patlak and Blasberg, 1985; Zhou et al, 2003; Zhou et al, 2009) was used to generate parametric V_T images. This novel graphic analysis method is a model-independent quantitative approach.

Bitopertin Plasma Concentration

On the days of the second and third PET scans, arterial blood samples were collected pre-scan and post-scan to determine the plasma concentrations of bitopertin. These were measured by a specific and validated liquid chromatography–mass spectrometry or mass spectrometry method.

Bitopertin Plasma Concentration–GlyT1 Occupancy Relationship

For the assessment of the relationship between bitopertin plasma concentration and GlyT1 occupancy, the mean of pre- and post-scan concentrations vs occupancy on the last day of treatment and after discontinuation were applied to a simple E_{max} model:

$$\text{Occ}\,(\%) = E_{max} \times C/(EC_{50} + C) \text{ OR Occ}$$
$$(\%) = E_{max} \times D/(ED_{50} + D)$$

where E_{max}: maximal occupancy (%), EC_{50}: half-maximal concentration (ng/ml), ED_{50}: half-maximal dose (mg), C: plasma concentration (ng/ml), and D: dose (mg). The analyses were performed using WinNonlin Professional version 5.2 (Pharsight Corporation, Mountain View, CA).

RESULTS

Subjects

Eighteen healthy male volunteers aged 20–51 years; with a body mass index of 19.5–29.3 kg/m^2 were enrolled. Five subjects were allocated to the 5 mg dose group, four to the

15 mg group and three each to the 30, 60, and 175 mg groups (Supplementary Table S1).

Five subjects withdrew prematurely for non-safety reasons. Fifteen subjects (three per dose group) had two evaluable scans, ie, at baseline and on the last day of bitopertin (RG1678) treatment. Thirteen subjects had three evaluable scans, ie, at baseline, under treatment, and after drug discontinuation.

[^{11}C]RO5013853 in Plasma and its Metabolite Ratio

In plasma, the metabolite ratio of [^{11}C]RO5013853 was $22.5 \pm 4.8\%$ (14.1–32.4%) and $45.0 \pm 5.5\%$ (35.4–57.2%) 30 and 90 min after injection, respectively (mean $\pm$ SD (range), $N = 40$, excluding subjects with baseline scan only). The ratio was comparable before and after bitopertin administration (Supplementary Figure S2).

The metabolite-corrected [^{11}C]RO5013853 activity in plasma had relatively low variation (Supplementary Figure S3). The mean coefficient of variation between 7 and 90 min after injection was 21.0% (range: 19.6–23.4%).

Bitopertin Plasma Concentration

Bitopertin steady-state plasma concentrations (mean of pre- and post-scan concentrations collected between 5 and 9 h post dose) increased in a dose-proportional manner. Following administration of 5, 15, 30, 60, or 175 mg bitopertin once daily for 10–12 days, plasma concentrations were 66.7 ± 5.2, 146 ± 26.8, 438 ± 47.0, 561 ± 135, and 1628 ± 298 ng/ml, respectively (mean $\pm$ SD, $N = 3$).

Two days after drug discontinuation (between 49 and 57 h after last dose) concentrations decreased to approximately half that of the respective concentrations reported on the last day of treatment, ie, to 32.8 ± 4.4 and 233 ± 50.9 ng/ml after 5 and 30 mg, respectively (mean $\pm$ SD, $N = 3$; dose groups with $N < 3$ not reported). This is in line with a terminal half-life of ~ 2 days.

Time–Activity Curves

TACs at baseline revealed a rapid initial decline in SUV, followed by a slower elimination phase in areas of high GlyT1 binding (Figure 1). SUV was highest in pons, thalamus, and cerebellum and lowest in cortical areas.

At steady state of a high bitopertin dose (175 mg once daily), TACs in the regions with high GlyT1 density were comparable with cortical areas, which was in line with a pronounced displacement of [^{11}C]RO5013853 by bitopertin.

Parameter Estimates Derived by 2T5P Model

At baseline, the transport rate constant from vascular space to target tissue, K_1, ranged from 0.028 to 0.045 ml/min/cm^3 and was uniform across all brain regions, except white matter where K_1 was ~ 0.019 (Supplementary Table S2). K_1 values remained uniform overall across the baseline and blocking scans, and thus were generally unaffected by bitopertin.

At baseline, regional V_T values were highest in the pons, thalamus, and cerebellum (1.7–2.7 ml/cm^3), intermediate to low in the putamen, caudate, and white matter (~ 1 ml/cm^3),
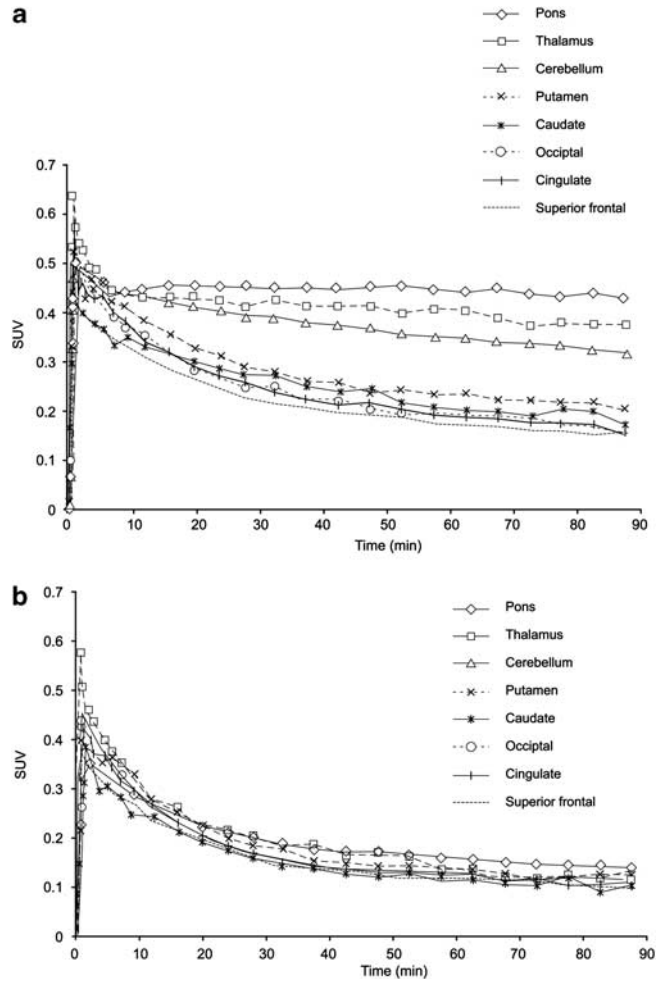
Figure 1 Time–activity curves of [^{11}C]RO5013853 in healthy volunteers at baseline (a) and at steady state of 175 mg bitopertin once daily (b; mean, $N = 3$). SUV = Average standardized uptake values. Time–activity curves of parietal, orbital frontal, prefrontal, and temporal cortices are similar to superior frontal cortex (curves not shown).

and lowest in cortical areas (~ 0.8 ml/cm^3). V_T values were reduced to a homogeneous level following administration of 175 mg bitopertin (Table 1). As V_T was low in superior frontal cortex and exhibited only a small decrease of 0.27 ml/cm^3 after administration of 60 or 175 mg bitopertin, ie, from 0.86 ± 0.05 to 0.59 ± 0.07 ml/cm^3 (mean $\pm$ SD, $N = 5$), it was chosen as the reference region.

At baseline, the binding potentials obtained by the 2T5P model in the pons, thalamus, and cerebellum were 2.19 ± 0.24, 1.49 ± 0.03, and 1.15 ± 0.17, respectively (mean $\pm$ SD, $N = 3$). At the steady state for 175 mg bitopertin, the binding potentials were reduced by five- to eight-fold to 0.42 ± 0.03, 0.20 ± 0.16, and 0.14 ± 0.05, respectively. The respective occupancy values were $80.4 \pm 3.8\%$, $86.7 \pm 10.7\%$, and $87.8 \pm 2.8\%$.

To assess the influence of reference region selection, occupancy was calculated for the pons, thalamus, and cerebellum using the orbital frontal, parietal, prefrontal, or temporal cortex values and compared with the results obtained using the superior frontal cortex as the reference region. The smallest difference was observed for the prefrontal cortex, where the median difference in occupancy

Table 1 V_T (volume of distribution, ml/cm^3) Values of [^{11}C]RO5013853 Derived by Two-tissue-five-parameter Model (2T5P) Model in Healthy Volunteers at Baseline and at Steady State of Different Bitopertin Doses Administered Once Daily

Region of interest	Time point	5 mg $N = 2$, values	15 mg $N = 3$, mean ± SD	30 mg $N = 3$, mean ± SD	60 mg $N = 2$, values	175 mg $N = 3$, mean ± SD
Pons	Baseline	3.011, 2.718	2.690 ± 0.071	2.615 ± 0.453	2.999, 3.037	2.627 ± 0.168
	Steady state	2.305, 1.588	1.886 ± 0.513	1.333 ± 0.448	1.102, 0.817	0.863 ± 0.019
Thalamus	Baseline	2.236, 2.331	2.074 ± 0.283	2.114 ± 0.272	2.311, 2.727	2.047 ± 0.042
	Steady state	1.680, 1.296	1.522 ± 0.323	1.162 ± 0.455	0.957, 0.688	0.727 ± 0.109
Cerebellum	Baseline	1.528, 1.904	1.721 ± 0.193	1.812 ± 0.286	2.088, 1.949	1.775 ± 0.174
	Steady state	1.378, 1.168	1.344 ± 0.377	1.014 ± 0.347	0.860, 0.647	0.693 ± 0.037
Putamen	Baseline	1.036, 1.088	1.064 ± 0.075	1.123 ± 0.176	1.159, 1.338	1.092 ± 0.079
	Steady state	0.941, 0.729	0.991 ± 0.211	0.841 ± 0.291	0.758, 0.594	0.700 ± 0.081
Caudate	Baseline	0.955, 0.958	0.986 ± 0.107	1.001 ± 0.140	0.950, 1.321	0.979 ± 0.105
	Steady state	0.865, 0.658	0.890 ± 0.251	0.788 ± 0.246	0.677, 0.473	0.617 ± 0.044
Occipital	Baseline	0.868, 0.900	0.860 ± 0.057	0.853 ± 0.083	0.989, 1.066	0.903 ± 0.076
	Steady state	0.885, 0.635	0.848 ± 0.201	0.756 ± 0.267	0.708, 0.550	0.663 ± 0.009
Cingulate	Baseline	0.862, 0.894	0.850 ± 0.033	0.856 ± 0.084	1.038, 0.983	0.893 ± 0.062
	Steady state	0.879, 0.627	0.826 ± 0.135	0.756 ± 0.273	0.700, 0.520	0.635 ± 0.014
Parietal	Baseline	0.830, 0.896	0.819 ± 0.028	0.817 ± 0.053	0.967, 0.975	0.849 ± 0.055
	Steady state	0.865, 0.631	0.821 ± 0.175	0.750 ± 0.249	0.717, 0.534	0.629 ± 0.014
Orbital frontal	Baseline	0.776, 0.846	0.810 ± 0.081	0.824 ± 0.083	0.984, 0.943	0.828 ± 0.007
	Steady state	0.790, 0.613	0.800 ± 0.210	0.737 ± 0.250	0.683, 0.539	0.615 ± 0.036
Prefrontal	Baseline	0.741, 0.767	0.793 ± 0.039	0.787 ± 0.074	0.917, 0.872	0.805 ± 0.027
	Steady state	0.768, 0.572	0.774 ± 0.167	0.695 ± 0.239	0.680, 0.489	0.602 ± 0.023
Temporal	Baseline	0.822, 0.865	0.800 ± 0.046	0.805 ± 0.061	0.956, 0.879	0.819 ± 0.044
	Steady state	0.815, 0.608	0.818 ± 0.174	0.749 ± 0.253	0.695, 0.510	0.629 ± 0.008
Superior frontal	Baseline	0.817, 0.798,	0.790 ± 0.030	0.772 ± 0.055	0.907, 0.923	0.823 ± 0.021
	Steady state	0.810, 0.576	0.777 ± 0.161	0.676 ± 0.238	0.671, 0.485	0.606 ± 0.010
Centrum semiovale	Baseline	0.925, 1.075	1.012 ± 0.120	0.984 ± 0.177	1.204, 1.061	0.983 ± 0.076
(white matter)	Steady state	0.992, 0.803	1.101 ± 0.310	0.915 ± 0.381	0.853, 0.660	0.803 ± 0.036

Scans without arterial line and subjects with baseline scan only were excluded.

was 0.7% (cerebellum, pons, thalamus, last day of treatment and 2 days after discontinuation pooled, $N = 75$ [occupancy$^{\text{test ref region}}$ − occupancy$^{\text{superior frontal cortex}}$]: 25th –75th percentile: − 1.3 to 3.3%). The largest difference was observed for the parietal cortex, where the mean difference was 3.9% (25th–75th percentile: 1.2–6.1%). Thus, GlyT1 occupancy derived by the 2T5P model is comparable whether the superior frontal, prefrontal, orbital frontal, temporal, or parietal cortex is used as reference region.

Parametric Images

Voxel-wise parametric mapping showed that the pons, thalamus, and cerebellum were the regions with the highest V_T, and that [^{11}C]RO5013853 could be displaced dose-dependently by bitopertin (Figure 2). This is consistent with the estimates of V_T derived by compartmental modeling.

Relationship Between Bitopertin Dose, Plasma Concentration And Occupancy Derived by 2T5P Model

At each dose level investigated, GlyT1 occupancy by bitopertin was similar between the pons, thalamus, and cerebellum both at steady state and 2 days after drug

discontinuation. At steady state, occupancy amounted to 30% (mean, range: 19–38%), 40% (32–48%), 60% (53–67%), 74% (70–79%), and 85% (74–94%) in the three areas after 5, 15, 30, 60, and 175 mg bitopertin, respectively (two subjects, three ROIs each for 5 and 60 mg; three subjects, three ROIs each for 15, 30, and 175 mg). Two days after drug discontinuation, occupancy decreased in all dose groups, as exemplified by 46% occupancy (38–56%) for the 30 mg dose.

At steady state, the bitopertin plasma concentration–occupancy relationship was well described by a simple $E_{\max}$ model with an $E_{\max}$ of ∼92% and an EC$_{50}$ of ∼190 ng/ml in the pons, thalamus, and cerebellum (Table 2). The ED$_{50}$ was ∼15 mg.

The relationship between plasma concentration and occupancy was superimposable at steady state and 2 days after drug discontinuation (Figure 3).

Comparison of 2T5P with SRTM and PRTM

GlyT1 occupancy was derived by the 2T5P model with arterial input function, the SRTM without arterial input function and the PRTM, which takes the region with the lowest target expression as the reference and makes a
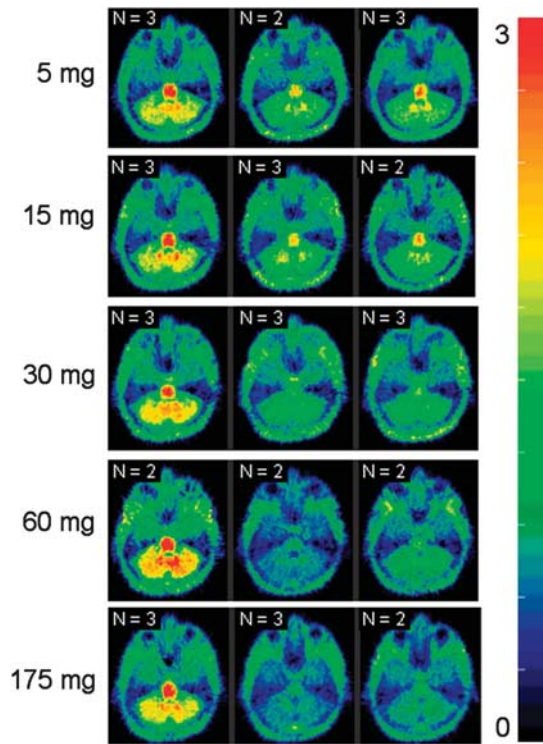
Figure 2 Composite parametric mean V_T (volume of distribution) images (midbrain, cerebellum) after intravenous administration of [^{11}C]RO5013853 to healthy volunteers at baseline (left), at steady state (middle), and 2 days after drug discontinuation (right) of varying bitopertin doses. N indicates number of subjects. The composite images include all subjects; however, scans without arterial line and subjects with baseline scan only were excluded.

Table 2 E_{max} and EC_{50} Values of Relationship Between Bitopertin Plasma Concentration[a] and GlyT1 Occupancy of Bitopertin at Steady State by Region of Interest and Model

Method	Region of interest	E_{max} (%)	EC_{50} (ng/ml)
2T5P	Cerebellum	99.4 (CV%: 4.1)	233 (CV%: 13.3)
	Pons	85.9 (CV%: 4.6)	156 (CV%: 17.0)
	Thalamus	92.2 (CV%: 5.9)	169 (CV%: 23.2)
SRTM	Cerebellum	97.2 (CV%: 4.8)	246 (CV%: 14.7)
	Pons	88.2 (CV%: 6.1)	209 (CV%: 19.8)
	Thalamus	90.1 (CV%: 6.1)	149 (CV%: 22.3)
PRTM	Cerebellum	98.8 (CV%: 3.3)	165 (CV%: 12.0)
	Pons	88.6 (CV%: 3.6)	114 (CV%: 15.1)
	Thalamus	91.6 (CV%: 5.0)	110 (CV%: 21.2)

Abbreviations: CV, coefficient of variation; EC_{50}, half-maximal concentration; E_{max}, maximal occupancy; PRTM, pseudoreference tissue model; SRTM, simplified reference tissue model; 2T5P, two-tissue five-parameter.
$N = 15$ for SRTM and $N = 13$ for 2T5P and PRTM.
[a]Mean of pre- and post-scan bitopertin plasma concentrations.

correction of the level of binding to this region (Gunn *et al*, 2011). The relationship between bitopertin plasma concentration and occupancy is shown in Figure 3.

The occupancy derived by SRTM was $\sim 2\%$ lower than the one calculated by the 2T5P model (cerebellum, pons, thalamus, last day of treatment and 2 days after discontinuation pooled, $N = 75$, median (occupancy^{SRTM} − occupancy^{2T5P}): − 2.2%, 25th to 75th percentile: − 5.3 to − 0.2%). The occupancy derived by PRTM was $\sim 7\%$ higher than the one calculated by the 2T5P model (median: + 7.1%, 25th to 75th percentile: + 5.5 to + 7.6%) with the largest difference occurring at an occupancy of 40–50% (Supplementary Table S3, Supplementary Figure S4).

Safety

Bitopertin doses of 5–175 mg administered for 10–12 days, and microdoses of [^{11}C]RO5013853 were well tolerated with no serious AEs. No AEs led to withdrawal from the study. There were no severe AEs. All AEs resolved without sequelae, except one case of unrelated wrist pain due to arterial line insertion where the subject was lost to follow-up.

There were 38 AEs reported by 10 out of 18 subjects across all dose groups, of which 26 were considered mild and 12 moderate. In the 5, 15, and 30 mg groups (12 subjects), all eight AEs were considered to be unrelated or remotely related to bitopertin. In the 60 mg dose group

(three subjects), 6 out of 12 AEs were possibly or probably related, and in the 175 mg dose group (three subjects), 13 out of 18 AEs were possibly or probably related to bitopertin. In line with the high bitopertin dose (> 8-fold above highest dose assessed in Phase III), there were several re-occurring AEs at 175 mg (headache, dizziness, fatigue, constipation, and insomnia). The most frequently observed AEs, considered as possibly or probably associated to bitopertin, were dizziness (one of three and two of three subjects after 60 and 175 mg, respectively) and fatigue (two of three and one of three subjects after 60 and 175 mg, respectively). After 60 mg dizziness occurred as a unique event, whereas after 175 mg dizziness was reported as a recurrent event in both subjects. Dizziness occurred at the beginning of treatment (day 1–day 4) and ceased under treatment, indicating tolerance.

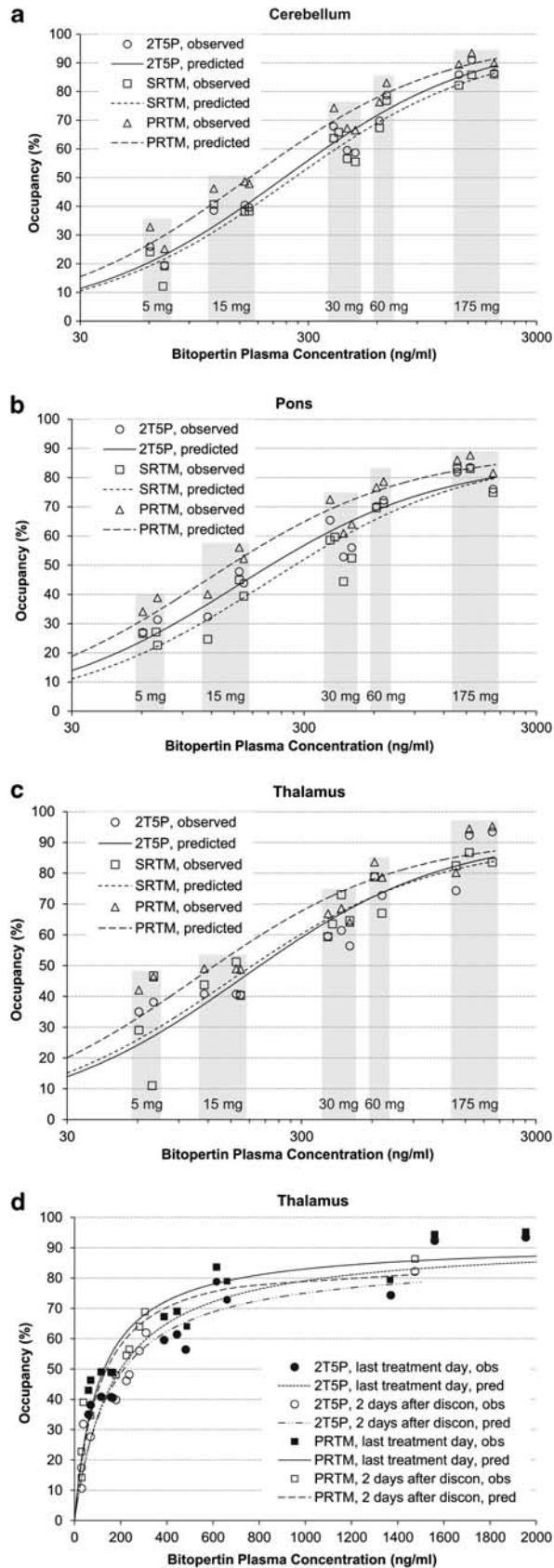There were no clinically relevant values or changes from baseline in vital signs, ECG or laboratory values.

DISCUSSION

[^{11}C]RO5013853

Regional [^{11}C]RO5013853 distribution volumes observed in this study (pons > thalamus > cerebellum » putamen ≈ caudate ≈ white matter > cortical areas, Table 1) are consistent with the known distribution of GlyT1 (Zafra *et al*, 1995; Cubelos *et al*, 2005), and the first human study with [^{11}C]RO5013853 (Wong *et al*, 2011), as well as autoradiographic studies with other GlyT1 tracers (ie, [^{11}C]GSK931145 (Herdon *et al*, 2010), [^{35}S]ACPPB (Zeng *et al*, 2008), and [^{18}F]MK-6577 (Hamill *et al*, 2011)).

SUV decreased three-fold in pons from ~ 0.45 at baseline to ~ 0.15 after administration of 175 mg bitopertin (RG1678) once daily, V_T decreased similarly by three-fold (ie, from ~ 2.6 to ~ 0.9 ml/cm^3), and binding potential five-fold from ~ 2.2 to ~ 0.4. The reduction in SUV is similar to that observed in a healthy volunteer study with [^{11}C]GSK931145, where SUV was reduced from ~ 1.5 to ~ 0.6 after a high GSK1018921 dose. However,

[¹¹C]GSK931145 has a high test–retest variability and the authors conclude that performance is 'at best moderate' (Gunn et al, 2011).

Figure 3 Relationship between bitopertin pre- and post-scan mean plasma concentration and GlyT1 occupancy in healthy volunteers on last day of treatment in the (a) cerebellum, (b) pons, and (c) thalamus, derived by two-tissue five-parameter (2T5P) model, simplified reference tissue model (SRTM), and pseudoreference tissue model (PRTM) as well as (d) on last day of treatment and 2 days after drug discontinuation in the thalamus. Bitopertin was administered once daily p.o. over 10–12 days at doses of between 5 and 175 mg. (a, b, c): gray areas represent bitopertin dose (d): one subject receiving daily doses of 175 mg bitopertin had the third scan 1 day instead of 2 days after the last dose. Accordingly, this subject displays higher occupancy ($\sim$80%) and plasma concentrations ($\sim$1480 ng/ml) after study drug discontinuation compared with the other subjects.

Selection of Reference Region

A valid reference region should exhibit no or negligible specific binding. As shown in Table 1, at dose levels around the ED_{50} of bitopertin (5–30 mg), V_T in the superior frontal cortex obtained under blocking conditions ($\sim$0.68–0.78 ml/cm^3) is comparable with V_T at baseline. V_T is slightly lower after 175 mg ($\sim$0.61 ml/cm^3), and after 60 mg ($\sim$0.58 ml/cm^3). The V_T results were verified by a model-independent graphical analysis using the Logan plot (Logan et al, 1990), where V_T was calculated as the slope of the linear portion of the Logan plot (40–90 min post tracer injection). The V_T of superior frontal cortex estimated accordingly was 0.97 ± 0.02 (mean $\pm$ SD) at baseline and decreased to 0.57 ± 0.11 ml/cm^3 at 60 mg.

The decrease in V_T of superior frontal cortex at higher dose levels could be due to the blocking of specific binding. We estimated the influence of the specific binding in the reference region on GlyT1 occupancy by applying PRTM (Gunn et al, 2011). PRTM uses the BP_{ND} of reference tissue estimated by the Lassen plot (Cunningham et al, 2010; Wong et al, 2000; Lassen et al, 1995), assuming that the distribution volume of free and nonspecific binding (V_{ND}) is the same across all ROIs, and that V_{ND} is the same between baseline and after treatments. On the basis of the Lassen plot, the BP_{ND} at baseline for the superior frontal cortex was 0.369 ± 0.392 (mean $\pm$ SD, $N = 25$). The occupancy values derived by PRTM were $\sim$7% higher than those obtained by 2T5P. Note that human autoradiographic studies indicate the presence of GlyT1 in cortical regions. However, GlyT1-specific binding is small in comparison with that measured in GlyT1-rich regions such as the thalamus and cerebellum (Borroni et al, 2011).

A reduction in SUV under blocked conditions in all brain regions, including the frontal cortex, was similarly observed in other studies (Hamill et al, 2011; Gunn et al, 2011). Although binding may be low in cortical areas, the small bitopertin binding observed may still be relevant for efficacy. Indeed GlyT1 has been found to be expressed not only in glial cells but also in neurons, particularly in glutamatergic neurons of cortex and hippocampus, whereas in more caudal brain regions it is predominantly expressed in glial cells surrounding glutamatergic synapses (Smith et al, 1992; Cubelos et al, 2005). In addition, the increased levels of extracellular glycine in rat striatum induced by bitopertin, as measured by microdialysis (Alberati et al, 2012), were similar to those reported for SSR504734, another GRI, where the microdialysis probe was implanted in medial prefrontal cortex (Depoortère et al, 2005).

Although 2T5P and PRTM find an overall comparable concentration–occupancy relationship, the slightly higher occupancy derived by PRTM is consistent with the small binding to GlyT1 detected in autoradiographic studies in cortical areas.

Bitopertin

Daily doses of 5–175 mg of bitopertin administered for 10–12 days were well tolerated. The bitopertin half-life is ~ 2 days, thus steady state was reached at the time point of the second PET scan. The relationship between plasma concentration and central GlyT1 occupancy derived by the 2T5P model, SRTM, and PRTM exhibited an EC_{50} of ~ 190, ~ 200, and ~ 130 ng/ml, respectively, in the pons, thalamus, and cerebellum, and was comparable to the value observed in monkeys (100–300 ng/ml; Borroni *et al*, 2011). For PRTM, the occupancy amounted to $\sim 48\%$ after 15 mg, ie, was close to the ED_{50}. E_{max} was $\sim 92\%$ independently of the model used.

For other psychotropic drugs (eg, quetiapine (Uppoor *et al*, 2008) or risperidone (Tauscher *et al*, 2002)), it was shown that the duration of occupancy is longer than anticipated, based on plasma concentration. For bitopertin, however, the concentration–occupancy relationship is superimposable at steady state and 2 days after discontinuation. Thus, bitopertin plasma concentration is a reliable predictor of occupancy.

Conclusions

This PET study in healthy volunteers showed that [^{11}C]RO5013853 is a suitable PET imaging agent for the GlyT1 transporter and assessment of occupancy by a GlyT1-specific drug. The described relationship between plasma concentration of bitopertin (RG1678), a GRI, and central GlyT1 occupancy allows understanding of the concentration–occupancy–efficacy relationship of bitopertin and supports dose selection of future molecules.

REFERENCES

Alberati D, Moreau JL, Lengyel J, Hauser N, Mory R, Borroni E *et al* (2012). Glycine reuptake inhibitor RG1678: a pharmacologic characterization of an investigational agent for the treatment of schizophrenia. *Neuropharmacology* **62**: 1152–1161.

Borroni E, Zhou Y, Ostrowitzki S, Alberati D, Kumar A, Hainzl D *et al* (2011). Pre-clinical characterization of [11C]R05013853 as a novel radiotracer for imaging of the Glycine Transporter type 1 by Positron Emission Tomography. *Neuroimage;* e-pub ahead of print 10 December 2011. doi:10.1016/j.neuroimage.2011.11.090.

Cubelos B, Giménez C, Zafra F (2005). Localization of the GLYT1 glycine transporter at glutamatergic synapses in the rat brain. *Cereb Cortex* **15**: 448–459.

Cunningham VJ, Matthews JC, Gunn RN, Rabiner EA, Gee AD (2004). Identification and interpretation of microparameters in neuroreceptor compartmental models. *Neuroimage* **22**(Suppl. 2): T13–T14.

Cunningham VJ, Rabiner EA, Slifstein M, Laruelle M, Gunn RN (2010). Measuring drug occupancy in the absence of a reference region: the Lassen plot re-visited. *J Cereb Blood Flow Metab* **30**: 46–50.

Depoortère R, Dargazanli G, Estenne-Bouhtou G, Coste A, Lanneau C, Desvignes C *et al* (2005). Neurochemical, electrophysiological and pharmacological profiles of the selective inhibitor of the glycine transporter-1 SSR504734, a potential new type of antipsychotic. *Neuropsychopharmacology* **30**: 1963–1985.

Friston K (2002). Statistical parametric mapping 2. http://www.fil.ion.ucl.ac.uk/spm/software/spm2/.

Gunn RN, Murthy V, Catafau AM, Searle G, Bullich S, Slifstein M *et al* (2011). Translational characterization of [((11)C) GSK931145, a PET ligand for the glycine transporter type 1 (GlyT1-1). *Synapse* **65**: 1319–1332.

Hamill TG, Eng W, Jennings A, Lewis R, Thomas S, Wood S *et al* (2011). The synthesis and preclinical evaluation in rhesus monkey of [(18)F]MK-6577 and [(11)C]CMPyPB, glycine transporter 1 positron emission tomography radiotracers. *Synapse* **65**: 261–270.

Herdon HJ, Roberts JC, Coulton S, Porter RA (2010). Pharmacological characterisation of the GlyT-1 glycine transporter using two novel radioligands. *Neuropharmacology* **59**: 558–565.

Hilton J, Yokoi F, Dannals RF, Ravert HT, Szabo Z, Wong DF (2000). Column-switching HPLC for the analysis of plasma in PET imaging studies. *Nucl Med Biol* **27**: 627–630.

Hofmann C, Alberati D, Banken L, Boetsch C, Ereshefsky L, Jhee S *et al* (2011). Glycine transporter type 1 (GlyT1) inhibitor RG1678: proof of mechanism of action in healthy volunteers. *Schizophr Bull* **37**(Suppl 1): 306.

Innis RB, Cunningham VJ, Delforge J, Fujita M, Giedde A, Gunn RN *et al* (2007). Consensus nomenclature for *in vivo* imaging of reversibly binding radioligands. *J Cereb Blood Flow Metab* **27**: 1533–1539.

Javitt DC (2006). Is the glycine site half saturated or half unsaturated? Effects of glutamatergic drugs in schizophrenia patients. *Curr Opin Psychiatry* **19**: 151–157.

Javitt DC (2007). Glutamate and schizophrenia: phencyclidine, N-methyl-D-aspartate receptors, and dopamine-glutamate interactions. *Int Rev Neurobiol* **78**: 69–108.

Javitt DC (2009). Glycine transport inhibitors for the treatment of schizophrenia: symptom and disease modification. *Curr Opin Drug Discov Devel* **12**: 468–478.

Koeppe RA, Holthoff VA, Frey KA, Kilbourn MR, Kuhl DE (1991). Compartmental analysis of [11C]flumazenil kinetics for the

estimation of ligand transport rate and receptor distribution using positron emission tomography. *J Cereb Blood Flow Metab* **11**: 735–744.

Lammertsma AA, Hume SP (1996). Simplified reference tissue model for PET receptor studies. *Neuroimage* **4**: 153–158.

Lassen NA, Bartenstein PA, Lammertsma AA, Prevett MC, Turton DR, Luthra SK et al (1995). Benzodiazepine receptor quantification *in vivo* in humans using [11C]flumazenil and PET: application of the steady-state principle. *J Cereb Blood Flow Metab* **15**: 152–165.

Logan J, Fowler JS, Volkow ND, Wolf AP, Dewey SL, Schlyer DJ et al (1990). Graphical analysis of reversible radioligand binding from time-activity measurements applied to [N-11C-methyl]-(-)-cocaine PET studies in human subjects. *J Cereb Blood Flow Metab* **10**: 740–747.

Patlak CS, Blasberg RG, Fenstermacher JD (1983). Graphical evaluation of blood-to-brain transfer constants from multiple-time uptake data. *J Cereb Blood Flow Metab* **3**: 1–7.

Patlak CS, Blasberg RG (1985). Graphical evaluation of blood-to-brain transfer constants from multiple-time uptake data. Generalizations. *J Cereb Blood Flow Metab* **5**: 584–590.

Pinard E, Alanine A, Alberati D, Bender M, Borroni E, Bourdeaux P et al (2010). Selective GlyT1 inhibitors: discovery of [4-(3-fluoro-5-trifluoromethylpyridin-2-yl)piperazin-1-yl][5-methanesulfonyl-2-((S)-2,2,2-trifluoro-1-methylethoxy)phenyl]methanone (RG1678), a promising novel medicine to treat schizophrenia. *J Med Chem* **53**: 4603–4614.

Pinard E, Burner S, Cueni P, Hartung T, Norcross RD, Schmid P et al (2011). Radiosynthesis of [5-[11C]methanesulfonyl-2-((S)-2,2,2-trifluoro-1-methyl-ethoxy)-phenyl]-[5-(tetrahydro-pyran-4-yl)-1,3-dihydro-isoindol-2-yl]-methanone ([11C]RO5013853), a novel PET tracer for the glycine transporter type I (GlyT1). *J Labelled Comp Radiopharm* **54**: 702–707.

Smith KE, Borden LA, Hartig PR, Branchek T, Weinshank RL (1992). Cloning and expression of a glycine transporter reveal colocalization with NMDA receptors. *Neuron* **8**: 927–935.

Tauscher J, Jones C, Remington G, Zipursky RB, Kapur S (2002). Significant dissociation of brain and plasma kinetics with antipsychotics. *Mol Psychiatry* **7**: 317–321.

Uppoor RS, Mummaneni P, Cooper E, Pien HH, Sorensen AG, Collins J et al (2008). The use of imaging in the early development of neuropharmacological drugs: a survey of approved NDAs. *Clin Pharmacol Ther* **84**: 69–74.

Wong DF, Nestadt G, Cumming P, Yokoi F, Gjedde A (2000). Partition volume and regional binding potentials of serotonin receptor and transporter ligands. In: Gjedde A, Hansen SB, Knudsen GM, Pavison OB (eds). *Physiological Imaging of the Brain with PET*. Academic Press: San Diego, pp 257–263.

Wong DF, Ostrowitzki S, Zhou Y, Raymont V, Hofmann C, Borroni E et al (2011). Characterization of [11C]RO5013853, a novel PET tracer for the glycine transporter Type 1 (GlyT1) in humans. *Neuroimage;* e-pub ahead of print 1 December 2011. doi:10.1016/j.neuroimage.2011.11.052.

Zafra F, Aragón C, Olivares L, Danbolt NC, Giménez C, Storm-Mathisen J (1995). Glycine transporters are differentially expressed among CNS cells. *J Neurosci* **15**: 3952–3969.

Zeng Z, O'Brien JA, Lemaire W, O'Malley SS, Miller PJ, Zhao Z et al (2008). A novel radioligand for glycine transporter 1: Characterization and use in autoradiographic and *in vivo* brain occupancy studies. *Nucl Med Bio* **35**: 315–325.

Zhou Y, Endres CJ, Brašić JR, Huang SC, Wong DF (2003). Linear regression with spatial constraint to generate parametric images of ligand-receptor dynamic PET studies with a simplified reference tissue model. *Neuroimage* **18**: 975–989.

Zhou Y, Resnick SM, Ye W, Fan H, Holt DP, Klunk WE et al (2007). Using a reference tissue model with spatial constraint to quantify [11C]Pittsburgh compound B PET for early diagnosis of Alzheimer's disease. *Neuroimage* **36**: 298–312.

Zhou Y, Ye W, Brašić JR, Crabb AH, Hilton J, Wong DF (2009). A consistent and efficient graphical analysis method to improve the quantification of reversible tracer binding in radioligand receptor dynamic PET studies. *Neuroimage* **44**: 661–670.

Zhou Y, Ye W, Brašić JR, Wong DF (2010). Multi-graphical analysis of dynamic PET. *Neuroimage* **49**: 2947–2957.

Supplementary Information accompanies the paper on the Neuropsychopharmacology website (http://www.nature.com/npp)